DALTON

A new two-dimensional manganese(II)–azide polymer. Synthesis, structure and magnetic properties of $[\{Mn(minc)_2(N_3)_2\}_n]$ (minc = methyl isonicotinate) †

Albert Escuer,*[a] Ramon Vicente,[a] Mohamed A. S. Goher*[b] and Franz A. Mautner[c]

[a] *Departament de Química Inorgànica, Universitat de Barcelona, Diagonal 647, 08028 Barcelona, Spain*
[b] *Chemistry Department, Faculty of Science, Kuwait University, PO Box 5969, Safat 13060, Kuwait*
[c] *Institut für Physikalische und Theoretische Chemie, Technische Universität Graz, A-8010 Graz, Austria*

A new two-dimensional manganese compound showing $\mu_{1,3}$-azido bridges has been synthesized and structurally characterised. The complex $[\{Mn(minc)_2(N_3)_2\}_n]$, where minc corresponds to methyl isonicotinate, crystallises in the monoclinic system, space group $P2_1/c$, $a = 12.424(5)$, $b = 8.496(3)$, $c = 8.399(4)$ Å, $\beta = 96.41(3)°$ and $Z = 2$. Magnetic measurements show behaviour typical of a two-dimensional Heisenberg antiferromagnet with $J = -2.24(2)$ cm^{-1}. Low-temperature properties are discussed in comparison with those of some molecular magnets of the $[\{MnL_2(N_3)_2\}_n]$ series.

The magnetochemistry of copper(II)[1] or nickel(II)[2] polynuclear compounds with azide as bridging ligand has markedly increased in the past few years, mainly due to the extreme versatility of this ligand to allow ferro- or antiferro-magnetic coupling according to the co-ordination mode (end-on or end-to-end) and also due to the possibility of tuning the magnetic properties by modifying the bond parameters of the bridging region.[3] Copper and nickel derivatives generally consist of discrete molecular compounds (di-,[2] tri-[4] or tetra-nuclear[5] systems), nickel chains[2] and some scarce examples of two-dimensional[6] compounds. In contrast, the practically unexplored manganese–azide system is currently attracting the attention of magnetochemists, since in addition to the above indicated properties it permits us to work with a greater local spin value and the manganese(II) system easily gives high-dimensional compounds. It is significant that only two discrete dinuclear[7,8] complexes $[NaMn(pyzc)(N_3)_2(H_2O)_2]$ (pyzc = pyrazine-2-carboxylate) and $[\{Mn(terpy)_2\}_2(\mu\text{-}N_3)_2X_2]$ (terpy = 2′,2′:6′,2″-terpyridine) have recently been reported, whereas the remaining compounds are chains[9] $[\{Mn(bpy)(N_3)_2\}_n]$ (bpy = 2,2′-bipyridine), two-dimensional systems $[\{Mn(pyca)(N_3)(H_2O)\}_n]$ (pyca = pyridine-2-carboxylate),[10] the series[11–13] $[\{MnL_2(N_3)_2\}_n]$ (L = 3-acetylpyridine, 4-acetylpyridine, ethyl isonicotinate or 4-cyanopyridine), three-dimensional compounds[13,14] $[\{Mn(py)_2(N_3)_2\}_n]$ (py = pyridine), $[NMe_4][\{Mn(N_3)_3\}_n]$ and the two isomeric[15,16] two- and three-dimensional compounds $[\{Mn_2(bipym)(N_3)_4\}_n]$ (bipym = 2,2′-bipyrimidine).

One of the most interesting properties of these two- and three-dimensional manganese–azide compounds is the spontaneous magnetisation at T_c between 16 and 40 K found for several $[\{MnL_2(N_3)_2\}_n]$ complexes.[13] Following our systematic exploration of these series we have prepared and structurally characterised the manganese derivative of the same general formula in which L = methyl isonicotinate. The magnetic behaviour indicates antiferromagnetic coupling, which has been explained in terms of the structural parameters according to the model previously reported. The low-temperature properties have been analysed in comparison with other previously reported two-dimensional antiferromagnetic systems.

† *Non-SI units employed*: G = 10^{-4} T, $\mu_B \approx 9.27 \times 10^{-24}$ J T^{-1}.

Experimental

Synthesis

An aqueous solution of sodium azide (0.455 g, 7 mmol) was added dropwise to a mixture of manganese chloride trihydrate (0.59 g, 3 mmol) and methyl isonicotinate (minc) (1.3 g, 10 mmol) in water–ethanol (1:1, 30 cm^3). The final clear solution was kept in a refrigerator for 2 weeks, yielding a yellow crystalline compound. Recrystallisation from hot water and very slow concentration on cooling for several weeks gave well formed yellow crystals of $[\{Mn(minc)_2(N_3)_2\}_n]$ suitable for X-ray determination. Yield *ca.* 60% [Found (Calc): C, 40.7 (40.57); H, 3.4 (3.27); Mn, 13.3 (13.62); N, 27.1 (26.87%)]. IR: bands corresponding to the methyl isonicotinate ligand [characteristic ν(CO) at 1730 cm^{-1}] and two well defined peaks at 2135 and 2051 cm^{-1} [$\nu_{asym}(N_3)$].

Spectral and magnetic measurements

Infrared spectra (4000–400 cm^{-1}) were recorded from KBr pellets on a Nicolet 520 FTIR spectrophotometer. Magnetic measurements were carried out with a Quantum Design instrument with a SQUID detector, working in the temperature range 2–300 K. The magnetic field was 100 G for the study of the low-temperature phenomena. Magnetisation measurements were recorded in the ±5 T range of external magnetic field. Diamagnetic corrections were estimated from Pascal tables. The EPR spectra were recorded at X-band frequency with a Bruker ES200 spectrometer equipped with an Oxford liquid-helium cryostat for variable-temperature work.

X-Ray crystallography

The X-ray single-crystal data were collected on a modified Stoe four-circle diffractometer. Crystal size: 0.60 × 0.35 × 0.28 mm. The crystallographic data, conditions for the collection of intensity data, and some features of the structure refinements are listed in Table 1. Graphite-monochromatised Mo-Kα radi-

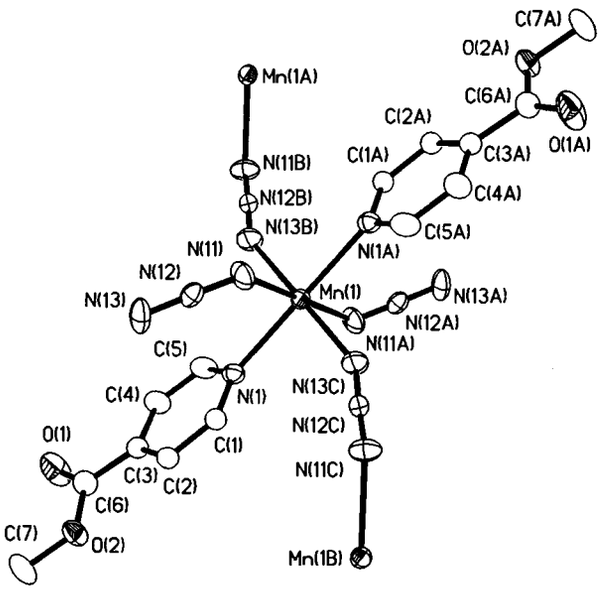

Fig. 1 Atom labelling scheme for $[\{Mn(minc)_2(N_3)_2\}_n]$

ation ($\lambda = 0.710\ 69$ Å) with the ω-scan technique was used to collect the data sets. The accurate unit-cell parameters were determined from automatic centring of 44 reflections ($5 < \theta < 16°$) and refined by least-squares methods. 2196 Reflections (1724 independent, R_{int} 0.0378) were collected in the range $3.30 < \theta < 26.49°$. Two reflections (4 1 1; 6 0 2) were collected every 45 min and used for intensity correction (intensity dropped continuously during data collection by 22%). Corrections were applied for Lorentz-polarisation effects, for intensity decay and also for absorption, using the DIFABS[17] computer program; range of normalised transmission coefficients 0.423–1.000. The structure was solved by direct methods using the SHELXS 86[18] computer program, and refined by full-matrix least-squares methods on F^2, using the SHELXL 93[19] program incorporated in the SHELXTL PC V 5.03[20] program library and the graphics program PLUTON.[21] All non-hydrogen atoms were refined anisotropically. The hydrogen atoms were located on calculated positions and assigned with one common isotropic displacement factor for each type of parent C atom. The final R factors were $R = 0.0548$ and $wR2 = 0.1317$. Number of refined parameters 127. Goodness of fit 1.061. Maximum and minimum peaks in the final difference synthesis were 0.485 and -0.457 e Å^{-3}. Significant bond parameters are given in Table 2.

CCDC reference number 186/714.

Results and Discussion

Crystal structure

The atom labelling scheme is shown in Fig. 1. The structure consists of an extended two-dimensional layer of octahedrally co-ordinated centrosymmetric manganese atoms, bridged by means of 1,3-μ-azide ligands, Fig. 2. Each manganese atom has two methyl isonicotinate ligands co-ordinated by means of the nitrogen atom of the pyridyl group in *trans* arrangement and four azide ligands in the equatorial plane. The axial Mn–N(1) bond distance is 2.304(2) Å whereas the slightly shorter Mn–N (azido) bond distances are Mn–N(11) 2.224(3) and Mn–N(13) 2.201(3) Å. Each of the four azide ligands acts as a $\mu_{1,3}$ bridge with each one of the neighbouring manganese atoms giving an extended two-dimensional layer. The bond angles Mn–N(11)–N(12) and Mn–N(13C)–N(12C) take the values 128.3(2) and 149.7(3)°, which lie in the normal M–N–N range found for $\mu_{1,3}$ bridges with copper, nickel or manganese polynuclear compounds. The torsion angle Mn–N–N–N–Mn, defined as the dihedral angle between the planes formed by the atoms Mn(1)–N(13C)–N(12C) and N(12C)–N(11C)–Mn(1B), is

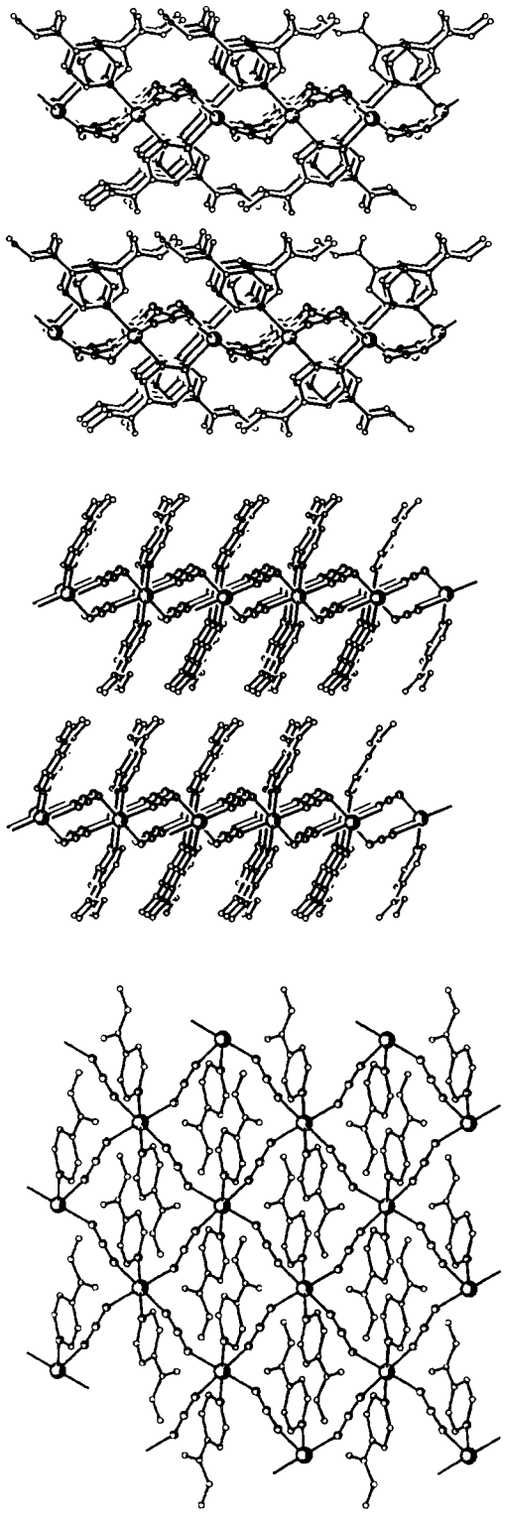

Fig. 2 Perspective view of $[\{Mn(minc)_2(N_3)_2\}_n]$ along the three main directions 0 0 1, 0 1 0 and 1 0 0

85.2(4)° and the acute interplanar angle between neighbouring MnN_4 planes is 84.9(1)°. The Mn · · · Mn shorter intraplane distances are 5.973(3) Å. The layers are well isolated by the *trans* methyl isonicotinate ligands, giving a minimum Mn · · · Mn interplane distance of 12.424 Å which corresponds with the x parameter of the cell.

It is interesting to compare the general trends of the present structure with those reported[11,22] for $[\{Mn(apy)_2(N_3)_2\}_n]$ (apy = 4-acetylpyridine) and $[\{Mn(NCS)_2(EtOH)_2\}_n]$ or the carboxylate derivatives[23,24] $[MnL_2(H_2O)_2]_n$ in which L = 4-chloro-2-methylphenoxyacetate or phenoxyacetate, for which the same structural motif has been found: *trans* arrangement around the

Table 1 Crystal data for $[\{Mn(minc)_2(N_3)_2\}_n]$

Chemical formula	$C_{14}H_{14}MnN_8O_4$
M	413.27
Crystal symmetry	Monoclinic
Space group	$P2_1/c$
a/Å	12.424(5)
b/Å	8.496(3)
c/Å	8.399(4)
β/°	96.41(3)
U/Å^3	881.0(6)
Z	2
T/K	295(2)
D_c, D_m/g cm^{-3}	1.558, 1.55(2)
μ(Mo-Kα)/cm^{-1}	7.89
$R(F_o)$ [a]	0.0548
$wR(F_o^2)$ [b]	0.1317

[a] $\Sigma||F_o| - |F_c||/\Sigma|F_o|$. [b] $\{\Sigma w[(F_o)^2 - (F_c)^2]^2/\Sigma w(F_o)^4\}^{\frac{1}{2}}$.

Table 2 Bond lengths (Å) and angles (°) for $[\{Mn(minc)_2(N_3)_2\}_n]$

Manganese environment			
Mn(1)–N(13C)	2.201(3)	Mn(1)–N(13B)	2.201(3)
Mn(1)–N(11)	2.224(3)	Mn(1)–N(11A)	2.224(3)
Mn(1)–N(1)	2.304(2)	Mn(1)–N(1A)	2.304(2)
Mn(1)···Mn(1B)	5.973(3)		
Azido bridge			
N(11)–N(12)	1.165(3)	N(12)–N(13)	1.162(4)
Methyl isonicotinate ligand			
N(1)–C(1)	1.340(4)	C(5)–N(1)	1.336(4)
C(1)–C(2)	1.372(4)	C(3)–C(6)	1.490(4)
C(2)–C(3)	1.381(4)	C(6)–O(1)	1.191(4)
C(3)–C(4)	1.384(4)	C(6)–O(2)	1.333(4)
C(4)–C(5)	1.377(5)	O(2)–C(7)	1.437(4)
Manganese and azide environment			
N(11)–Mn(1)–N(11A)	180.0	N(12)–N(11)–Mn(1)	128.3(2)
N(11)–Mn(1)–N(1)	88.2(1)	N(12C)–N(13C)–Mn(1)	149.7(3)
N(11)–Mn(1)–N(1A)	91.8(1)	C(1)–N(1)–Mn(1)	122.5(2)
N(11)–Mn(1)–N(13B)	91.4(1)	C(5)–N(1)–Mn(1)	119.2(2)
N(11)–Mn(1)–N(13C)	88.6(1)	N(13B)–Mn(1)–N(1A)	91.8(1)
N(11A)–Mn(1)–N(1)	91.8(1)	N(13C)–Mn(1)–N(1)	91.8(1)
N(11A)–Mn(1)–N(1A)	88.2(1)	N(13C)–Mn(1)–N(1A)	88.2(1)
N(11A)–Mn(1)–N(13B)	88.6(1)	N(13C)–Mn(1)–N(13B)	180.0
N(11A)–Mn(1)–N(13C)	91.4(1)	N(1A)–Mn(1)–N(1)	180.0
N(13B)–Mn(1)–N(1)	88.2(1)	N(13)–N(12)–N(11)	176.9(3)
Methyl isonicotinate ligand			
N(1)–C(1)–C(2)	123.5(3)	C(4)–C(3)–C(6)	118.9(3)
C(1)–C(2)–C(3)	118.9(3)	C(2)–C(3)–C(6)	122.9(3)
C(2)–C(3)–C(4)	118.1(3)	C(3)–C(6)–O(1)	124.5(3)
C(3)–C(4)–C(5)	119.3(3)	C(3)–C(6)–O(2)	112.1(3)
C(4)–C(5)–N(1)	122.9(3)	O(1)–C(6)–O(2)	123.5(3)
C(5)–N(1)–C(1)	117.3(3)	C(6)–O(2)–C(7)	116.4(3)

manganese atom and four azide, thiocyanate or carboxylate bridges respectively, to the four neighbouring manganese atoms. Comparative magnetic properties are discussed below.

Magnetic results

Plots of the molar magnetic susceptibility and the $\chi_M T$ product *vs.* T (for manganese) are shown in Fig. 3. The overall behaviour corresponds to a moderate antiferromagnetic coupling, showing a maximum of susceptibility at 24 K and a regular decay of $\chi_M T$ from room temperature (3.75 cm^3 K mol^{-1}) down to zero at low temperature. The χ_M value at low temperature tends to a finite value close to 0.033 cm^3 mol^{-1}. This finite value indicates the absence of paramagnetic impurities in the sample.

The high-temperature susceptibility data at 300–20 K were fitted by the expansion series[25] of Lines for an $S = \frac{5}{2}$ anti-

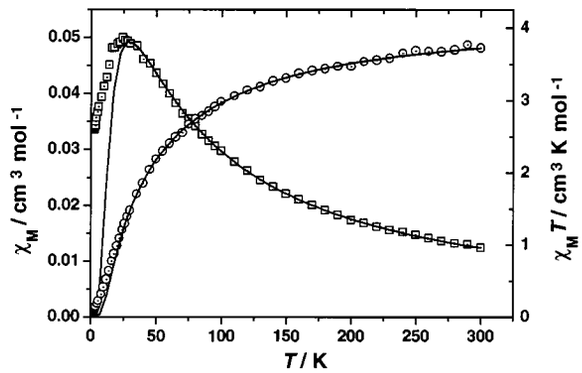

Fig. 3 Plots of χ_M (⊡) and $\chi_M T$ (⊙) *vs.* T for a polycrystalline sample of $[\{Mn(minc)_2(N_3)_2\}_n]$. The solid lines show the best fit under the conditions described in the text

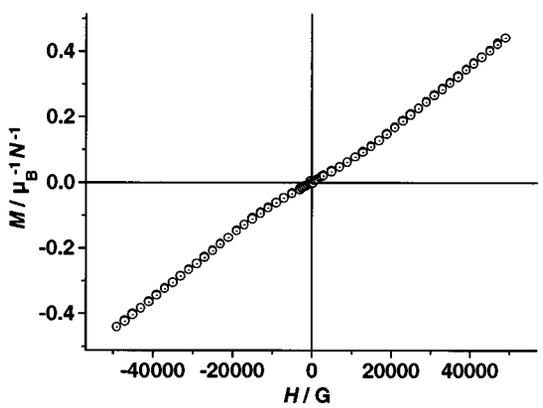

Fig. 4 Magnetisation at 2.5 K *vs.* applied field for $[\{Mn(minc)_2(N_3)_2\}_n]$

ferromagnetic quadratic layer, based on the exchange Hamiltonian $H = \Sigma_{nn} -JS_i \cdot S_j$ where Σ_{nn} runs over all pairs of nearest-neighbour spins i and j, equation (1) in which $\theta = kT/|J|S(S+1)$, $C_1 = 4$, $C_2 = 1.448$, $C_3 = 0.228$, $C_4 = 0.262$, $C_5 = 0.119$, $C_6 = 0.017$ and N, g and μ_B have their usual meanings. The best fit is given by the superexchange parameter $J = -2.24(2)$ cm^{-1}. This agrees with the value of $J = -2.37$ cm^{-1} expected from the position of the maximum given by expression[25] (2).

$$Ng^2\mu_B{}^2/\chi|J| = 3\theta + (\Sigma C_n/\theta^{n-1}) \quad (1)$$

$$kT_{max}/J = 1.12S(S+1) + 0.10 \quad (2)$$

A magnetisation experiment at 2.5 K under an external field in the ±5 T range, shows a normal behaviour for an antiferromagnetic two-dimensional system, without spontaneous magnetisation at zero field or hysteresis, Fig. 4.

The EPR spectrum measured on a polycrystalline powder at room temperature shows a sharp isotropic signal centred at $g = 2.000$, linewidth 46 G. The spectra measured at variable temperature are practically identical in the range 300–25 K, but when the temperature falls below the susceptibility maximum the intensity of the signal also decreases whereas the linewidth increases strongly: 103 at 15, 143 at 10 and finally 426 G at 4 K.

The magnetic properties of $[\{ML_2(N_3)_2\}]_n$ compounds may be studied in two well characterised regions: one, the paramagnetic phase that comprises the range between room temperature and the temperature close to the maximum of susceptibility and second, the low-temperature region. In the present case the high-temperature range may be reasonably assumed as 300–24 K. The overall pattern of the susceptibility data corresponds to an antiferromagnetic coupling, in agreement with the typical behaviour of $\mu_{1,3}$-azido bridges. The superexchange parameter $J = -2.24$ cm^{-1} is only comparable

Table 3 Some structural and magnetic properties for compounds of the $[\{MnL_2(N_3)_2\}_n]$ series. Compounds for which Δ_{pp} (4 K) are not reported correspond to those in which the EPR signal vanishes immediately after the three-dimensional order; cpy = 4-cyanopyridine; einc = ethyl isonicotinate

L	py	cpy	3-apy	4-apy	einc	minc
Azide type	$\mu_{1,3}$	$\mu_{1,1}/\mu_{1,3}$	$\mu_{1,1}/\mu_{1,3}$	$\mu_{1,3}$	$\mu_{1,1}/\mu_{1,3}$	$\mu_{1,3}$
Intersheet *d*/Å	[a]	13.579	11.843	11.563	15.760	12.424
Angle between manganese planes/°	64.6	20.9	81.9	83.3	67.5	84.9
T_C/K	40	18	16	28	16	—
Hysteresis loop	No	No	Yes	Yes	Yes	No
EPR Δ_{pp} (r.t.)	26.3	40	51	32.2	45.3	46
(4 K)	150 [b]	936	561	300 [c]	80	426
Ref.	15	15	15	13	14	This work

r.t. = Room temperature. [a] Three dimensional. [b] At 33 K. [c] At 30 K.

with the $J = -3.83$ cm^{-1} value obtained[13] for $[\{Mn(apy)_2(N_3)_2\}_n]$ which shows the same general pattern of four end-to-end azido bridges in a two-dimensional compound. The lowest value obtained for $[\{Mn(minc)_2(N_3)_2\}_n]$ is a good test of the recent proposal[12] about the superexchange through end-to-end azido bridges: the Mn–N–N bond angles show comparable values but the Mn–NNN–Mn torsion angle is greater in the present compound, allowing lower coupling. Therefore, the value of -2.24 cm^{-1} is also consistent with the proposal that, even for torsion angles close to 90°, the antiferromagnetic superexchange pathways provided by the t_{2g} orbitals of manganese(II) (d^5) are active, in contrast with the case of copper(II) or nickel(II) (d^9 and d^8), for which torsion angles close to 90° allow no coupling. This hypothesis seems also consistent with the greater value of -11.9 cm^{-1} found for the double azide-bridged compound[9] $[Mn(bpy)(N_3)_2]$ which show a lower torsion angle of 41.1°.

The low-temperature region differs from that of the previously reported $[\{Mn(apy)_2(N_3)_2\}_n]$ compound for which order was achieved at 28 K (from susceptibility data): $[\{Mn(apy)_2(N_3)_2\}_n]$ shows an increase of the EPR linewidth when the temperature decreases (signal vanishes at 30 K), shows magnetic hysteresis and spontaneous magnetisation at zero field below T_C. In the present case the EPR signal also changes with T at low temperatures (25–4 K) but does not vanish, even at 4 K (Table 3). The susceptibility plot shows anomalous behaviour at low temperature because it does not tend to zero when T tends to zero (χ_M value at 2 K is 0.033 cm^3 mol^{-1}) which indicates that magnetic ordering needs lower temperature in this case. Consistent with the previous data, magnetisation experiments performed at 2.5 K do not show spontaneous magnetisation at zero field nor magnetic hysteresis at ±5 T magnetic field.

The magnetic properties of the present compound may be compared with those of other two-dimensional manganese(II) systems that show low antiferromagnetic coupling and for which magnetic ordering is not yet achieved at the lowest limit of the measurement temperature. For $[\{Mn(NCS)_2(EtOH)_2\}_n]$ the superexchange parameter J takes the value -1.22 cm^{-1} and the low-temperature EPR spectra show an increase in the linewidth at low temperature, but the susceptibility plot does not show important deviations from the theoretical two-dimensional susceptibility plot even at low temperature, in a similar fashion to the magnetic properties of the carboxylate derivatives $[\{Mn(RCO_2)_2(H_2O)_2\}_n]$ which show J values close to -0.30 cm^{-1} and for which the most significant low-temperature property is also the increase in the linewidth of the EPR signal. For $[\{Mn(minc)_2(N_3)_2\}_n]$ ($J = -2.24$ cm^{-1}) the low-temperature susceptibility plot deviates from the ideal two-dimensional behaviour but does not achieve magnetic ordering properties (at least down to 2 K). This is consistent with the relation between the critical temperature and J (greater J gives greater T_C). The family of $[\{MnL_2(N_3)_2\}_n]$ complexes offers similar properties to those of the M_2MnF_4 (M = Rb or K)[25] systems and an important increase in T_C may be expected for lower torsion angles in contrast with thiocyanate or carboxylate bridges which, in all reported cases, allow weak antiferromagnetic coupling.

Acknowledgements

A. E. and R. V. thank the Comisión Interministerial de Ciencia y Tecnologia (Grant PB093/0772) for support of this research. F. A. Mautner thanks Professor C. Kratky (University of Graz) for use of experimental equipment.

References

1 S. Sikorav, I. Bkouche-Waksman and O. Kahn, *Inorg. Chem.*, 1984, **23**, 490; Y. Agnus, R. Louis, J. P. Gisselbrecht and R. Weiss, *J. Am. Chem. Soc.*, 1984, **106**, 93 and refs. therein.
2 J. Ribas, M. Monfort, B. K. Ghosh, R. Cortés, X. Solans and M. Font-Bardia, *Inorg. Chem.*, 1996, **35**, 864 and refs. therein.
3 J. Ribas, M. Monfort, C. Diaz, C. Bastos and X. Solans, *Inorg. Chem.*, 1993, **32**, 3557; A. Escuer, R. Vicente, J. Ribas, M. S. El Fallah, X. Solans and M. Font-Bardia, *Inorg. Chem.*, 1994, **33**, 1842; L. K. Thompson, S. S. Tandon and M. E. Manuel, *Inorg. Chem.*, 1995, **34**, 2356.
4 A. Escuer, I. Castro, F. A. Mautner, M. S. El Fallah and R. Vicente, *Inorg. Chem.*, in the press.
5 J. Ribas, M. Monfort, R. Costa and X. Solans, *Inorg. Chem.*, 1993, **32**, 695.
6 J. Ribas, M. Monfort, X. Solans and M. Drillon, *Inorg. Chem.*, 1994, **33**, 742.
7 M. A. S. Goher, F. A. Mautner and A. Popitsch, *Polyhedron*, 1993, **12**, 2557.
8 R. Cortés, L. Pizarro, L. Lezama, M. S. Arriortua and T. Rojo, *Inorg. Chem.*, 1994, **33**, 2697.
9 R. Cortés, L. Lezama, J. L. Pizarro, M. I. Arriortua, X. Solans and T. Rojo, *Angew. Chem., Int. Ed. Engl.*, 1994, **33**, 2488; R. Cortés, M. Drillon, X. Solans, L. Lezama and T. Rojo, *Inorg. Chem.*, 1997, **36**, 677.
10 M. A. S. Goher, M. A. M. Abu-Youssef, F. A. Mautner and A. Popitsch, *Polyhedron*, 1992, **11**, 2137.
11 A. Escuer, R. Vicente, M. A. S. Goher and F. A. Mautner, *Inorg. Chem.*, 1995, **34**, 5707.
12 A. Escuer, R. Vicente, M. A. S. Goher and F. A. Mautner, *Inorg. Chem.*, 1996, **35**, 6386.
13 A. Escuer, R. Vicente, M. A. S. Goher and F. A. Mautner, *Inorg. Chem.*, 1997, **36**, 3440.
14 F. A. Mautner, R. Cortés, L. Lezama and T. Rojo, *Angew. Chem., Int. Ed. Engl.*, 1995, **35**, 78.
15 G. De Munno, M. Julve, G. Viau, F. Lloret, J. Faus and D. Viterbo, *Angew. Chem., Int. Ed. Engl.*, 1996, **35**, 1807.
16 R. Cortés, L. Lezama, J. L. Pizarro, M. I. Arriortua and T. Rojo, *Angew. Chem., Int. Ed. Engl.*, 1996, **35**, 1810.
17 N. Walker and D. Stuart, *Acta Crystallogr., Sect. A*, 1983, **39**, 158.
18 G. M. Sheldrick, SHELXS 86, Program for the Solution of Crystal Structure, University of Göttingen, 1986.
19 G. M. Sheldrick, SHELXL 93, Program for the Refinement of Crystal Structure, University of Göttingen, 1993.
20 SHELXTL 5.03 (PC Version), Program library for the Solution and Molecular Graphics, Siemens Analytical Instruments Division, Madison, WI, 1995.
21 A. L. Spek, PLUTON 92, University of Utrecht, 1992.
22 J. N. McElearney, L. L. Balagot, J. A. Muir and R. D. Spence, *Phys. Rev.*, 1979, **19**, 306.
23 V. Tangoulis, G. Psomas, C. Dendrinou-Samara, C. P. Raptopoulou, A. Terzis and D. Kessissoglou, *Inorg. Chem.*, 1996, **35**, 7655.
24 G. Smith, E. J. O'Reilly and C. H. L. Kennard, *J. Chem. Soc., Dalton Trans.*, 1980, 2462.
25 M. E. Lines, *J. Phys. Chem. Solids*, 1970, **31**, 101.

Received 2*nd April* 1997; *Paper* 7/02214J